Research on dynamic obstacle avoidance method of autonomous vehicle for moving sub-targets

Liu Hao*, Hashimah Ismail, Nazlin Hanie binti Abdullah

Faculty of Engineering and Life Sciences, Universiti Selangor (UNISEL), Selangor 40000 , Malaysia

Abstract: Due to the uncertainty of vehicle position changes during driving, traditional obstacle avoidance methods have many limitations in terms of vehicle obstacle avoidance accuracy, and the actual application effect is difficult to meet the requirements of autonomous driving. In order to solve this problem, the vehicle obstacle avoidance strategy is updated and adjusted in real time in combination with the characteristics of mobile sub targets, so as to better adapt to the changes of uncertainty and make the auto drive system more reliable and accurate in the obstacle avoidance process. Firstly, during the driving process of autonomous vehicles, a comprehensive analysis and planning of the entire path are carried out to obtain global obstacle distribution information on the road segment; Then, establish a moving sub target motion model and uniformly optimize parameters and variables; Next, design a gradient guided dynamic obstacle avoidance reward function to optimize the accuracy of mobile sub objective decision-making; Finally, generate the optimal obstacle avoidance free path. Through performance comparison testing of the proposed method, the data shows that the method can effectively improve the vehicle's ability to handle unexpected factors and ensure safe passage of obstacles. The optimization effect is stable and easy to operate.

Keywords: autonomous vehicles; moving sub-targets; Dynamic obstacle avoidance; Methodological research

0. Introduction

Intelligent vehicles have made significant progress in perception, decision-making, and control, but currently there is no method to achieve high-precision avoidance of moving sub targets in the driving process. The reason for this is that the algorithms currently used in perception, decision-making, and control operations cannot complete the calculation and analysis of sudden factors in a short period of time [1-2], thereby increasing the probability of collisions between autonomous vehicles and obstacles.

To solve such problems, a dynamic obstacle avoidance method for autonomous vehicles towards moving sub targets is proposed based on the characteristics of moving targets. Firstly, obtain the distribution information of obstacles on the global road segment through global path analysis. Next, establish a motion model for moving sub targets and uniformly optimize relevant parameters and variables. Then, a gradient guided dynamic obstacle avoidance reward function is designed to improve the accuracy of mobile sub target decision-making. Finally, based on the comprehensive consideration of the above steps, the optimal obstacle avoidance free path is generated. The innovation of this method lies in the organic combination of global path analysis, mobile sub target motion optimization, and gradient guided reward function design, achieving dynamic obstacle avoidance optimization for mobile sub targets. The application of this method helps to improve the safety and efficiency of autonomous vehicle in various driving environments. By optimizing obstacle avoidance strategies and making precise decisions, the risk of collisions and accidents can be reduced, and overall driving efficiency can be improved. This method can make significant contributions to the development of autonomous driving technology, whether in complex driving scenarios such as urban roads or highways.

1. Specific study of obstacle avoidance parameters

1.1 Global path analysis for autonomous vehicles

The obstacle avoidance action of autonomous vehicles towards obstacles ahead during driving is a composite global path planning process [3-4]. Therefore, in order to ensure the accuracy of obstacle avoidance actions, it is first necessary to analyze the global path. Set the path and driving direction of the autonomous vehicle, and set a moving reference point along its direction. The autonomous vehicle tracks the reference point to achieve global path condition analysis. For ease of calculation, a method is proposed to use the reference point as a local target in global path analysis, and guide the form according to its reference direction to obtain a dynamic sub target point.

As shown in Figure 1, in the calculated and analyzed route R, set the road condition obstacle variable as $s(s \succ 0)$, and correspond to the route reference point, and the subscript t represents the travel time. Assuming that there is a dynamic sub-target point $P(s)$ on the path, the distance between the autonomous vehicle and the dynamic sub-target point is p, the tangent vector of the path corresponding to the dynamic sub-target point is $P'(s)$, and the projection of the tangent vector along the direction of the x and y axes can be expressed as $P'_x(s)$, $P'_y(s)$, (x, y, θ) represents the location coordinates of the autonomous vehicle, respectively, corresponding to the x-axis coordinates and y-axis coordinates of the autonomous vehicle in the world coordinate system and the orientation angle θ of the direction of the autonomous vehicle driven by the corresponding axis.

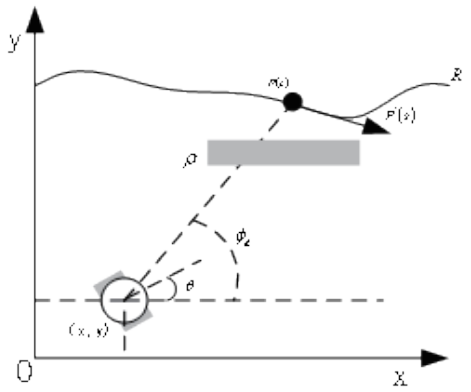

Figure 1 Road condition obstacle avoidance analysis

It can be seen that the control objectives of autonomous vehicles are shown in equations (1) and (2), that is, the forward distance of autonomous vehicles at random time points is less than the threshold d_ρ, and the angle formed between θ and $_d$ shall not be greater than or equal to the current threshold d_ρ, and its relationship function can be expressed as:

$$\rho(t) \prec d_\rho \quad (1)$$

$$f_{abs}(\theta - \phi_d) \leq d_\theta \quad (2)$$

In the equation， $f_{abs}(\theta-\phi_d)$ is the absolute value of the coefficient corresponding to $(\theta-\phi_d)$；ϕ_d represents the orientation angle formed between the position of the dynamic sub-target point and the autonomous vehicle; d_θ represents the maximum allowable lateral deviation in the path condition，which is generally set according to the path curvature and the acceleration of the autonomous vehicle[5][6].

If the actual moving speed of the dynamic sub-target in the world coordinate system is set to s_v，it can be represented by calculating the coefficient of change of s，as shown in equation (4). Where $\|\vec{c}'\|$ represents the modulus of the tangent vector coefficient at the location point as shown in equation (5). According to the constraint conditions for the relationship between equations (1) and (2)，the calculation formula for the driving speed $\dot{s}$ of the dynamic sub-target point $P(s)$ can be obtained as follows:

$$\dot{s}=\frac{e^{-\rho}\upsilon_n}{\sqrt{P_x'(s)^2+P_y'(s)^2}} \quad (3)$$

$$s_v=\dot{s}\|\vec{c}'\| \quad (4)$$

$$\|\vec{c}'\|=\sqrt{P_x'(s)^2+P_y'(s)^2} \quad (5)$$

In the formula: υ_n represents the actual driving speed of the autonomous vehicle; $c=e^{\alpha d_\rho}$；c represents the tangent vector coefficient; α represents the guiding coefficient，whose value is determined based on historical experience; The angular velocity ω_{ref} and linear velocity V_{ref} of autonomous vehicles driving to the dynamic sub-target point position can reflect the global path condition，and the corresponding calculation formula is:

$$\omega_{\text{ref}}=k\Delta\phi+\dot{\phi}_d \quad (6)$$

$$V_{\text{ref}}=p\cos(\Delta\phi) \quad (7)$$

In the formula: γ represents the maximum allowable tangential guidance error when the autonomous vehicle drives to the target position，$\gamma=\frac{\upsilon_n}{d_\rho}$；$\Delta\phi$ represents the angular bias coefficient，$\Delta\phi=\phi_d-\theta$；$\dot{\phi}_d$ represents the obstacle avoidance derivative corresponding to ϕ_d；k represents the proportional value of angular deviation.

Through the analysis of equations (6) and (7)，it can be seen that the angle deviation coefficient between the autonomous vehicle and the target angle ϕ_d is more closely related，the larger the

γ correspondence coefficient value, the smaller the distance deviation between the autonomous vehicle and the dynamic sub-target ρ, and the higher the success rate of vehicle obstacle avoidance.

1.2 Moving sub-target motion model construction

Based on the above dynamic sub-target analysis results, the motion model of moving sub-target is constructed to obtain an accurate description of the obstacle avoidance ability of autonomous vehicles for moving targets. Without considering the influence of road bump factors, dynamic air flow resistance factors, and ground lateral friction factors[7][8], the optimization design is carried out by the double-degree-of-freedom kinematics model[9][10] of the moving sub-target motion model of autonomous vehicles, as shown in Figure 2.

The constraints of the dynamic equation for moving sub-targets in the inertial coordinate system in which the vehicle sits under acceleration can be described as:

$$\frac{d}{dt}\begin{bmatrix} X_r(t) \\ Y_r(t) \\ \varphi(t) \\ v_1(t) \\ \delta(t) \end{bmatrix} = \begin{bmatrix} v_1(t)\cos\varphi(t) \\ v_1(t)\sin\varphi(t) \\ \dfrac{v_1(t)\tan\delta(t)}{L_w} \\ a(t) \\ \omega(t) \end{bmatrix} \quad (8)$$

where $\omega(t)$ represents the instantaneous velocity of the deflection angle corresponding to the front wheel of the autonomous vehicle; $a(t)$ represents the acceleration in the direction consistent with the x-axis; L_w represents the front and rear wheelbase of autonomous vehicles.

Considering that the variable control of the motion state of the moving sub-target needs to complete a manifold restriction operation in the solution space[11][12], the constraint interval of the control variable is defined as follows:

$$\begin{cases} |\delta(t)| \le \delta_{\max} \\ |a(t)| \le a_{x\max} \\ |v_1(t)| \le v_{\max} \\ |\omega(t)| \le \Omega_{\max} \end{cases}, t \in [0, t_f] \quad (9)$$

where $t_f \ge 0$; $a_{\max}$ and $\Omega_{\max}$ represent the linear acceleration, the amplitude of the maximum speed corresponding to the rotation angle of the front wheel, and the $\Omega_{\max}$ coefficient value is set to 1 according to the design needs; $v_{\max}$ represents the maximum speed of an autonomous vehicle during obstacle avoidance at low speeds; $\delta_{\max}$ represents the maximum rotation angle of the front wheel.

Based on the dynamic model, the moving sub-target obstacle is modeled:

$$\begin{bmatrix} \dot{x} \\ \dot{y} \end{bmatrix} = \begin{bmatrix} v_{obs}\cos\varphi_{obs} \\ v_{obs}\sin\varphi_{obs} \end{bmatrix} \quad (10)$$

where v_{obs} represents the mean velocity and φ_{obs} represents the obstacle avoidance heading angle.

The vehicle global analysis results are integrated with the sub-target obstacle dynamic model to

obtain the MZQV control system model[13][14] after various parameter correlations, and the Euler discrete integral calculation is used to obtain the final moving sub-target motion model:

$$[z(k+1)]=[z(k)]+\Delta t[f(z,u)] \quad (11)$$

where z represents the global parametric association state set; u represents the obstacle avoidance control factor.

To verify the model constructed above, it is assumed that an autonomous vehicle needs to avoid a moving pedestrian. Obtain road obstacle information through global path analysis, and then establish a dual degree of freedom motion model for pedestrians, taking into account the limitations of acceleration and motion direction. Integrate the global path and motion model into the MZQV control system model, and calculate the final moving sub target motion model through Euler discrete integration. This model can help vehicles accurately predict pedestrian movement trajectories and make corresponding decisions to avoid collisions.

1.3 Design of dynamic obstacle avoidance reward function for gradient guidance

In order to avoid the problem of large deviation of close obstacle avoidance by traditional obstacle avoidance methods, the proposed method maps the environmental state to the obstacle avoidance action model by enhancing the learning of moving sub-targets, and then obtains an optimal external state evaluation. Through continuous training between correction and mapping, a complete reward mechanism is formed, that is, when the vehicle correctly adjusts the obstacle avoidance direction, it will be given a positive reward; When the vehicle mistakenly adjusts the direction of obstacle avoidance, it will be given a negative reward. The process is expressed by sparse function. In order to avoid that the expression of sparse function is not conducive to the convergence control of the overall algorithm, the gradient guidance method is adopted to solve the problem on the constraint variables, and then the reward function with gradient guidance attribute in the dynamic obstacle avoidance process is obtained:

$$r_t = r_t^g + r_t^c + r_t^t + r_t^d + r_t^a \quad (12)$$

The reward function consists of five variables, where r_t^g represents the reward for the autonomous vehicle approaching the end goal:

$$r_t^g = \begin{cases} r^g & \|p_t - g\| \prec 0.3 \\ 0 & otherwise \end{cases} \quad (13)$$

r_t^c represents the penalty for autonomous vehicle obstacle avoidance failure:

$$r_t^c = \begin{cases} r^c & \text{If there is a collision risk} \\ 0 & otherwise \end{cases} \quad (14)$$

The r_t^t table represents the rewards for non abnormal time points during the driving process of autonomous vehicles:

$$r_t^t = \begin{cases} r^t & \|p_t - g\| \succ 0.3 \\ 0 & otherwise \end{cases} \quad (15)$$

r_t^d is set as gradient guidance of the distance of dynamic target obstacle avoidance, which is used to describe the effect of the coefficient of change between the position of the autonomous vehicle and the distance to the end point on the reward:

$$r_t^d = \begin{cases} \eta\left(\|p_t - g\| - \|p_{t-1} - g\|\right) & \|p_t - g\| \succ 0.3 \\ 0 & otherwise \end{cases} \quad (16)$$

The r_t^a is set as a gradient guide of the angle formed between the vehicle and the obstacle during obstacle avoidance, and is used to describe the effect of the angle change coefficient formed by the connection between the course of the autonomous vehicle and its end point on the reward:

$$r_t^a = \begin{cases} \beta\left|\angle p_t g - \angle p_{t-1} g\right| & \left|\angle p_t g - \angle p_{t-1} g\right| \succ 0.9 \\ 0 & otherwise \end{cases} \quad (17)$$

Among them, p_t represents the coordinates of the mobile autonomous vehicle at the moment, g represents the coordinates corresponding to the end point of the autonomous vehicle, η represents the gradient guidance coefficient of the dynamic distance, β represents the gradient guidance coefficient of the obstacle avoidance angle. According to the design needs and combined with historical experience, make the following Settings: $r^g = 3$, $r^c = -3$, $r^t = -0.0$, $\eta = -2$, $\beta = -0.2$, the radius of influence of the position of the moving target end point is 0.6, and the peak value of gradient guidance setting limit of obstacle avoidance Angle is 0.9. In Equation (17), $\angle p_t g$ is the angle formed by the connection between the line velocity direction of the autonomous vehicle and its end point at this moment. It can be seen from Equations (16)-(17) that the gradient guidance of distance and gradient guidance of angle in the design reward function reward and punishment for the driving autonomous vehicle are mainly determined according to the positive and negative values of the corresponding coefficient of the distance gradient and the angle gradient mentioned above, so as to promote the obstacle avoidance direction of the autonomous vehicle to be corrected in the direction with the smallest error distance from the obstacle target, and improve the obstacle avoidance accuracy and convergence speed of the algorithm.

By designing a dynamic obstacle avoidance reward function, the learning ability of autonomous vehicles towards moving sub targets has been enhanced. This reward function includes a reward term for vehicles approaching the destination, a penalty term for obstacle avoidance failure, and a reward term for non abnormal time points. Using gradient guidance method, gradient guidance coefficients for distance and angle are introduced into the reward function to encourage the vehicle to correct towards the direction closer to the obstacle and minimize angle deviation, thereby improving the accuracy and convergence speed of obstacle avoidance.

1.4 Generate an optimal obstacle avoidance free path

Based on the above calculation, combined with the dynamic characteristics of the moving sub-target obstacle, the optimal obstacle avoidance free path is generated. The specific process is as follows:

Taking the straight line in the direction of the obstacle avoidance angle ϕ_T of the moving sub-

target as the boundary, the coordinate plane where the global autonomous vehicle is located is divided into two parts in order from left to right, and the left and right half coordinate planes of the plane where the autonomous vehicle is located are obtained. The unconstrained sector closest to ϕ_T in the two half-plane coordinate planes is the region with the dynamic optimal obstacle avoidance of the moving sub-target, which is called the optimal obstacle avoidance free sector. Thus, the optimal obstacle avoidance free path ϕ_s can be selected in this region. Let the adjacent barrier area O_i , O_j (O_i represents the barrier area range, i, j represents the barrier area range boundary) contain a free sector, the left and right boundary angles corresponding to the free sector are θ_l , θ_r , then the width angle $\theta = |\theta_l - \theta_r|$. Considering the difference in the size of θ , the following two situations can be summarized based on historical experience to select the optimal obstacle avoidance free path ϕ_c .

(1) When $\theta_{\text{mid}} \succ \theta \succ \theta_{\min}$ is satisfied, there is one narrow free sector between O_i and O_j that allows autonomous vehicles to safely avoid obstacles. where $\theta_{\min}$ and θ_{mid} represent two preset parameters, $\theta_{\min}$ represents the minimum value of free sector angle under the safe obstacle avoidance condition of autonomous vehicle, and θ_{mid} represents the coefficient value corresponding to the free sector angle under the condition of obstacle avoidance under the normal state of no adjustment of the autonomous vehicle. Considering that narrow spaces under the condition of free sector obstacle avoidance are prone to path oscillation[15] and affect the obstacle avoidance effect, a multi-path alternative is adopted in the obstacle avoidance path planning of this sector, and the free path ϕ_c is randomly selected at the middle line of the free sector and is satisfied as follows:

$$\phi_c = \frac{\theta_l + \theta_r}{2} \quad (18)$$

(2) When $\theta \geq \theta_{\text{mid}}$ is satisfied, there is a huge obstacle avoidance free sector between O_i and O_j . There are no collision factors in this sector, and the path where the autonomous vehicle is located during the passage will not cause oscillation, so the corresponding angle of the straight line where the boundary of the free sector is located is selected as an alternative path, so that two free paths ϕ_{c1} and ϕ_{c2} can be obtained to ensure that the autonomous vehicle can accurately move along the boundary of the obstacle area, namely:

$$\left.\begin{aligned}\phi_{c1} = \theta_l \\ \phi_{c2} = \theta_r\end{aligned}\right\} \quad (19)$$

As shown in Figure 2, expanding the search in the figure yields the optimal free sectors 1, 4 in the left and right planes. Among them, the alternative free paths are ϕ_{c1} , ϕ_{c2} , ϕ_{c3} .

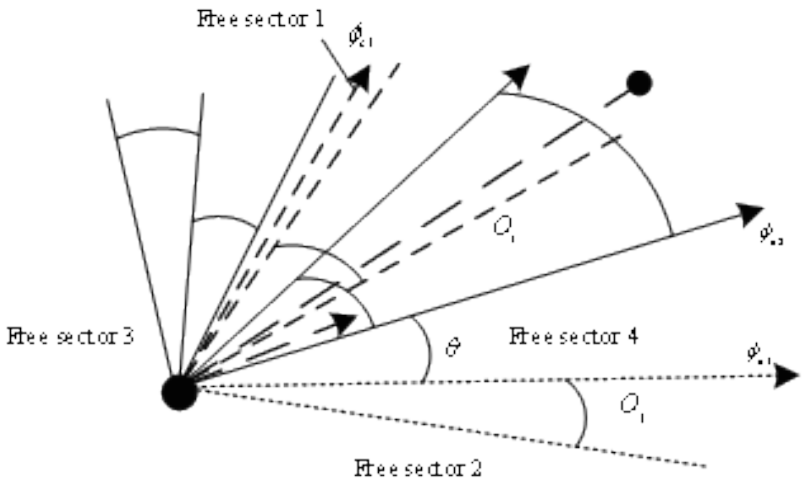

Figure 2 Free path determination

Through the dynamic obstacle avoidance cost function shown in Equation (20), all the selected alternative obstacle avoidance free paths ϕ_i are evaluated one by one, and the least cost path evaluated is set to the optimal obstacle avoidance free path ϕ_s. Taking the determined optimal path as the obstacle avoidance guidance of the autonomous vehicle, the dynamic obstacle avoidance cost function of the successful obstacle avoidance area process of the progressive sub-target of the autonomous vehicle can be obtained as follows:

$$C(\phi_c)=k_1\Delta(\phi_c,\phi_T)+k_2\Delta(\phi_c,\phi_{s-1})+k_3\Delta(\phi_c,\phi_v) \quad (20)$$

In the formula: C represents the dynamic obstacle avoidance cost coefficient; ϕ_c represents the radial angle information of the alternative free path introduction; ϕ_{s-1} represents the radial angle corresponding to the optimal free path in the previous calculation process; k_1, k_2, k_3 represent 3 positive integers; The function $\Delta(,)$ represents the minimum coefficient of the angle amplitude formed by randomly selecting the polar axis where the two angular values are located.

2. Application testing

The proposed research method was tested, and the test used the method of multi-method index acquisition in the same environment, obtaining relevant performance indicators, and analyzing them to obtain test results. Based on the above settings, two different obstacle avoidance methods were introduced as references, labeled as Reference-1 and Reference-2, respectively. The proposed method is marked as Verification-0.

2.1 Set test conditions

The simulation test tool MATLAB was used to simulate a test section with a length of 150 m. Dynamic obstacles are simulated by laser collection points on the road section, and the obstacle point and the test vehicle are driven at a constant speed at their respective speeds. The instantaneous acceleration of the test vehicle and obstacle point is not considered during the test. The specific test parameters are shown in Table 1.

Table 1 Simulation scenario configuration parameters

Control parameters	Control quantity	Control parameters	Control quantity
Obstacle coordinates	[2,5,1]	Obstacle avoidance angle control threshold	0.003
Edge coordinates	[1,1,1]	Rotation angle	0.5
Rotational angular coordinates	(2.3)	Maximum control coefficient	28
Obstacle avoidance deviation control quantity	1.5	Maximum bias coefficient	16
Maximum speed per hour	15m/s	Acceleration	20

2.2 Proximity obstacle avoidance response test

Three sets of different obstacle distance data were generated as test samples under the set parameters, with distances of 30m, 20m and 10m, respectively. Obstacle avoidance tests were carried out by 3 different methods, and the instantaneous response time of each method was recorded. The shorter the response time, the higher the obstacle recognition degree of the corresponding method. Conversely, the longer the response time, the lower the obstacle recognition degree of the corresponding method. The test results are shown in Figure 3.

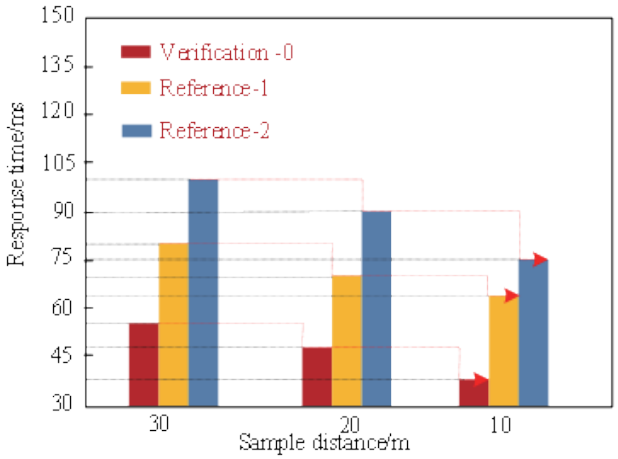

Figure 3 Obstacle avoidance response results obtained at different distances by different obstacle avoidance methods

According to the data comparison shown in Figure 3, it can be seen that there is a significant difference in the performance of the three different obstacle avoidance methods at different obstacle distances. However, each method exhibits good consistency in performance, as the distance between the test vehicle and the obstacle point decreases, the obstacle avoidance response time decreases to adapt to the processing of obstacle avoidance actions. Among them, the obstacle avoidance response time of validation −0 is less than 60ms, while the overall obstacle avoidance response time of reference −1 and reference −2 is higher than 65ms. From this, it can be concluded that this method can maintain consistent and good obstacle avoidance performance in the presence of obstacles at different distances. As the obstacle distance decreases, it can respond more quickly, demonstrating a high degree of obstacle recognition ability.

2.3 Obstacle avoidance effect test

Three sets of obstacle points are randomly set on the set lane, and the obstacle avoidance operation is operated by three different methods, and the rationality of the obtained obstacle avoidance path of each obstacle avoidance method is compared, then the test conclusion is obtained. The distribution of obstacle points and the test results are shown in Figure 4−6.

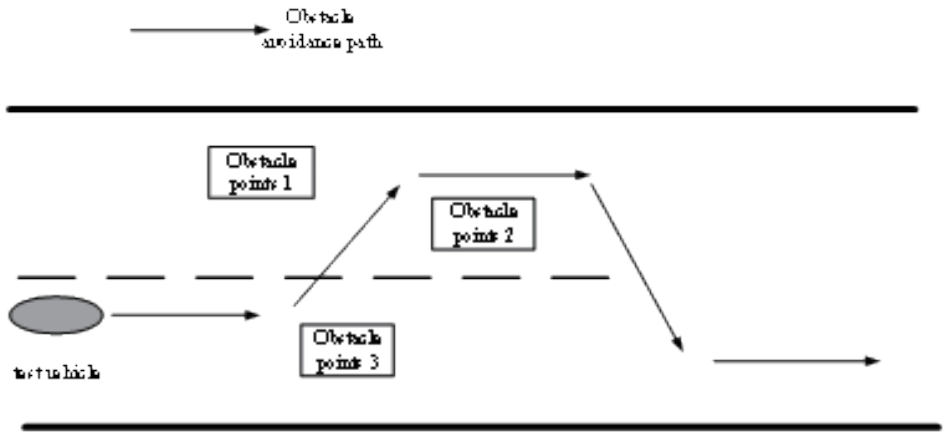

Figure 4 Reference-1 obstacle avoidance path planning

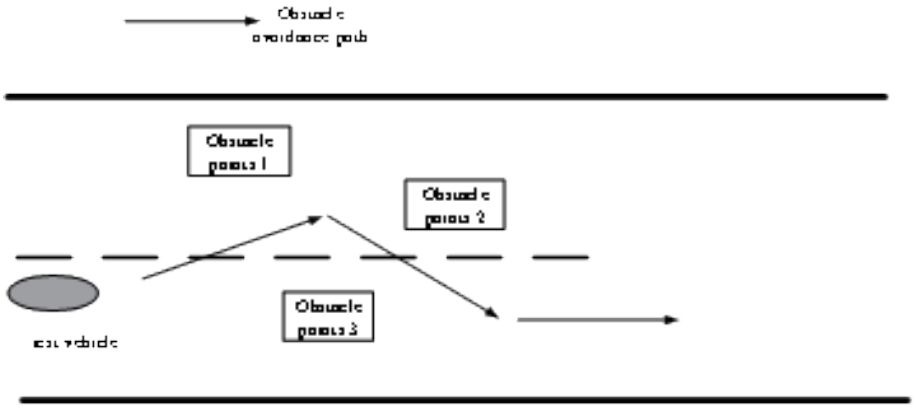

Figure 5 Reference-2 obstacle avoidance path planning

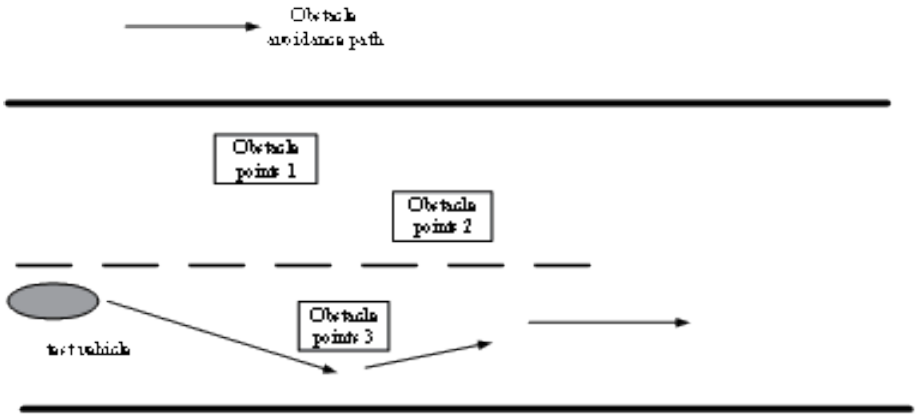

Figure 6 Verification-0 obstacle avoidance path planning

By comparing Figure 4-6, it can be seen that the obstacle avoidance path planned by Reference-1 in Figure 4 is the longest, and there are unnecessary actions; In Figure 5, the distance of the obstacle avoidance path planned with Reference-2 is reasonable, but there are also unnecessary obstacle avoidance actions, and the obstacle avoidance safety factor is low. The obstacle avoidance path planned by Verification-0 in Figure 6 has a short distance, no unnecessary obstacle avoidance actions, and the safety factor of the entire obstacle avoidance line is high. Based on the above comparative analysis, it can be determined that the obstacle avoidance effect of Verification-0 is the best.

3. Conclusion

By dynamically analyzing and calculating the process parameters of obstacle avoidance for moving sub targets, this method optimizes the obstacle path determination mechanism of vehicles,

improves the accuracy of vehicle obstacle avoidance for moving obstacles, and further improves the success rate of vehicle safety obstacle avoidance. The proposal of this method enriches the current solutions for vehicle obstacle avoidance problems. However, there are still some potential shortcomings, such as accuracy issues in close range vehicle recognition responses and obstacle avoidance actions. In order to further improve this method, future research can consider introducing intelligent algorithms such as network IoT technology to reduce the probability of defect occurrence and optimize the reliability and safety of autonomous driving technology. Therefore, this method enriches vehicle obstacle avoidance solutions, but still needs to focus on areas for improvement to achieve more reliable and safe autonomous driving technology.

References:

[1] Cui Yuding, Xiong Haojie, He Manchuan, et al. Autonomous driving active obstacle avoidance strategy based on Model predictive control [J/OL]. Agricultural Equipment & Vehicle Engineering: 1-7 [2023-06-10].

[2] Zhang Liping, Zhao Junmei, Liu Dan, et al. Research on Obstacle Avoidance and Trajectory Planning Simulation Technology Based on Grid Tracking [J]. Vehicle & Power Technology, 2023 (02): 36-42.

[3] Zhao Ying, Zhang Qi, Yu Ting, et al. Research on path planning method for obstacle avoidance of intelligent vehicles [J]. Journal of Nanjing University of Science and Technology, 2023,47 (02): 148-154.

[4] Liu Cunxiang, Liu Xuejun, Lin Tugan, et al. Design and testing of steering brake obstacle avoidance control strategy for unmanned new energy vehicles [J]. Small Internal Combustion Engine and Vehicle Technique, 2023,52 (02): 67-71.

[5] Jiang Nan, Xu Jian. Research on obstacle avoidance algorithm for unmanned vehicles based on extended Kalman filter [J]. Computer Knowledge and Technology, 2023,19 (08): 16-18+25.

[6] Feng Guoyu, Wang Xiaogang, Xu Hui, et al. Design of a real-time obstacle avoidance decision-making method for edge vehicles [J]. Journal of Fujian Computer, 2023,39 (03): 21-25

[7] Xu Jingxian. Obstacle avoidance trajectory planning for autonomous vehicles [J]. Automobile Applied Technology, 2023,48 (04): 9-13.

[8] Liu Qian, Qiu Guansheng, Zeng Zhaoyu. Improved A~* Algorithm for Automatic Driving Path Planning by Integrating DWA Algorithm [J]. Automation & Instrumentation, 2023 (02): 32-36+41.

[9] Zhan Qi, Zhou Wei, Li Wenliang, et al. Fuzzy comprehensive evaluation of vehicle intelligent lane changing and obstacle avoidance function based on combination weighting [J]. Journal of Highway and Transportation Research and Development, 2023,40 (01): 236-244.

[10] Teng Ruipin. Path algorithm for obstacle avoidance of automatic driving based on turning motion geometry [J]. Journal of Changsha Social Work College, 2022,29 (04): 127-132.

[11] Zhong Zuoteng, Zhou Jianfu, Zhou Jingyu, et al. Identification and Control Strategies for Obstacle Avoidance Scenarios in Networked Collaborative Driving [J]. Information & Computer, 2021,33 (24): 172-174.

[12] Wei Lingtao, Wang Xiangyu, Qiu Bin, et al. Tracking and obstacle avoidance control of autonomous vehicles based on adaptive preview path [J]. Journal of Mechanical Engineering, 2022,58 (06): 184-193.

[13] Li Xiaoyu, Xu Jiyang, Ma Fei. Research on a path planning method for autonomous obstacle avoidance [J]. Agriculture and Technology, 2021,41 (15): 57-59.

[14] Hua Zuxu, Zhang Wenhai. Obstacle avoidance path planning for autonomous vehicle based on Bessel curve [J]. Automotive Digest, 2021 (07): 46-49.

[15] Li Ning, Wei Deng, Cao Yujie, et al. Obstacle avoidance control algorithm for autonomous electric vehicles [J]. Chinese Journal of Scientific Instrument, 2021,42 (05): 199-207.